



# Measurement of 3D Displacement fields using 3D Laser and CCD Camera

Rahel Rahel, Mussa Mahmud, Roy Michael, Jean François Fontaine

## ► To cite this version:

Rahel Rahel, Mussa Mahmud, Roy Michael, Jean François Fontaine. Measurement of 3D Displacement fields using 3D Laser and CCD Camera. 7th International Working CIRP Conference - Total Quality Management - Advanced and Intelligent Approaches, Jun 2013, Belgrade, Serbia. pp.212-216. hal-00907140

**HAL Id: hal-00907140**

**<https://hal.science/hal-00907140>**

Submitted on 20 Nov 2013

**HAL** is a multi-disciplinary open access archive for the deposit and dissemination of scientific research documents, whether they are published or not. The documents may come from teaching and research institutions in France or abroad, or from public or private research centers.

L'archive ouverte pluridisciplinaire **HAL**, est destinée au dépôt et à la diffusion de documents scientifiques de niveau recherche, publiés ou non, émanant des établissements d'enseignement et de recherche français ou étrangers, des laboratoires publics ou privés.

## MEASUREMENT OF 3D DISPLACEMENT FIELDS USING 3D LASER SCANNER AND CCD CAMERA

UDC: 006.91; 65.012.7 ; 544.144.2 ; 514.747

**Rahel Rahel<sup>1</sup>, Mussa Mahmud<sup>1</sup>, M. Roy Michaël<sup>2</sup>, Jean-François Fontaine<sup>2</sup>**

<sup>1</sup> Faculty of Mechanical Eng., Omar AL-MAKTAR University, Tobruk- Libya

<sup>1</sup> Faculty of Mechanical Eng., AL-TAHADI University, Sirte- Libya

<sup>2</sup> Laboratoire d'Electronique, Informatique et Image(Le2I), UMRCNRS 5158 Université de Bourgogne, site d'Auxerre-France.

[Rahelmar@yahoo.fr](mailto:Rahelmar@yahoo.fr)

Paper received: 24.02.2013.; Paper accepted: 20.03.2013.

**Abstract:** Many applications dealing with the mechanical behavior of materials require the measurement of displacement fields or deformation fields. For this type of measurement, optical methods have become unavoidable due to their non-intrusive approach, their high spatial resolution, their high sensitivity, the large size of their examined field, and the increasing power of the computers that now allow the processing of huge quantities of data. In this context we have developed a system for measuring 3-D displacement fields using CCD camera and 3D laser scanner. This method allows the measure of the 3-D displacement field using at least two pairs of stereoscopic images of an object corresponding to two states of its deformation (or the processing of a sequence of pairs of images acquired during the deformation). The main topics developed in this thesis are: the calibration of a camera and a 3D laser scanner, and measuring 3D displacement fields from coupling of camera and 3D laser sensor. The potential application of our method is the characterization of structures, for example, to provide assistance in the development of tools for stamping.

**Key Words:** : camera calibration, measuring 3-D displacement fields, 3D laser sensor calibration, non-contacting 3-D metrology.

### 1. INTRODUCTION

Optical methods for measuring displacement are now widely used in mechanical experiments. The main techniques are photoelasticity, geometric moiré, moiré interferometry, holographic interferometry, speckle interferometry (speckle), the grid method and digital image correlation [4, 5, 6, 7, 10, 12]. Method of digital image correlation (DIC) is probably one of the most commonly used, many applications of DIC method are presented by R. HORAUD [12], and more specifically for the measurement of displacement fields from 3D stereo coupling and monitoring-correlation of pixels in a sequence of images by correlation [1, 2, 3].

When only one camera is used, the DIC can give the displacement field only in the planar domain of the observed object. Otherwise using a camera accompanied with a laser sensor 3D, can be measure the displacement field in the 3D surface.

In this study we use the camera and an image correlation method to define the displacement field of a moving object. The coupling of the camera and the 3D scanner allows us to associate the observed displacement field and the 3D surface of the object. The measured displacements are on the 3D surface of the order of 20mm to 40mm.

### 2. Camera calibration and 3D scanner

#### 2.1. Calibration parameters of the camera

The calibration of a camera is to determine the coordinates (u, v) in the image coordinate system b from the coordinates (x, y, z) in the coordinate B world. In other words, it consists in solving the following equation:

$$b = M_c(B) \quad (1)$$

To do this, we must first express B in the camera frame, and then calculate the coordinates of b in the same spot after a projection. Finally, changes in the b mark image plane for its coordinates (u, v).

##### 2.1.1. Determination of b from

To calculate the coordinates of b in the image plane from point B whose coordinates are expressed in the reference world.

$$\begin{pmatrix} su \\ sv \\ s \end{pmatrix} = M_c \begin{pmatrix} x \\ y \\ z \\ 1 \end{pmatrix} \quad (2)$$

$$\text{Where } M_c = \begin{pmatrix} m_{11} & m_{12} & m_{13} & m_{14} \\ m_{21} & m_{22} & m_{23} & m_{24} \\ m_{31} & m_{32} & m_{33} & m_{34} \end{pmatrix}$$

In this equation, the coordinates are homogeneous. The homogeneous coordinates of the object point B (x, y, z, 1), and those of the pixel b is

( $su, sv, s$ ). Cartesian coordinates of  $b$  are ( $su/s, sv/s$ ). is the perspective projection matrix. Using equation (2), However, we can write the Cartesian coordinates of an image point as shown in Equation (3).

$$u = \frac{m_{11}x + m_{12}y + m_{13}z + m_{14}}{m_{31}x + m_{32}y + m_{33}z + m_{34}}$$

$$v = \frac{m_{21}x + m_{22}y + m_{23}z + m_{24}}{m_{31}x + m_{32}y + m_{33}z + m_{34}}$$

### 2.1.2. Calculating calibration parameters $Y$

The calibration parameters can be obtained from the perspective projection matrix  $M_C$ . We apply the method to calculate Faugeras-Toscani  $M_C$  [8,9].

The calibration parameters of a camera intrinsic parameters to include  $a_u, a_v, u_0, v_0$  and extrinsic parameters  $R$  and  $T$ . These parameters can be calculated from the perspective projection matrix  $M_C$

Equation (4) shows how to calculate the calibration parameters from the  $M_C$  matrix [11]

$$r_3 = m_3$$

$$u_0 = m_1 \cdot m_3$$

$$v_0 = m_2 \cdot m_3$$

$$au = -\|m_1 \wedge m_3\|$$

$$av = \|m_2 \wedge m_3\|$$

$$r_1 = 1/a_u (m_1 - u_0 m_3)$$

$$r_2 = 1/a_v (m_2 - v_0 m_3)$$

$$t_x = 1/a_u (m_{14} - u_0 m_{34})$$

$$t_y = 1/a_v (m_{24} - v_0 m_{34})$$

$$t_z = m_{34}$$
(4)

### 2.2. Method for 3D laser sensor calibration

The 3D scanner is composed of a sensor and a laser sheet coordinate measuring machine. It helps to have a dense cloud of points with an accuracy of the order of 10 microns. The calibration pattern is used marble cube whose faces are perpendicular. Two checkerboard patterns as were positioned on the faces oriented along the X and Y directions of the machine. Each level of the target is represented by a cloud of points ( $x, y, z$ ) (see Figure 1).

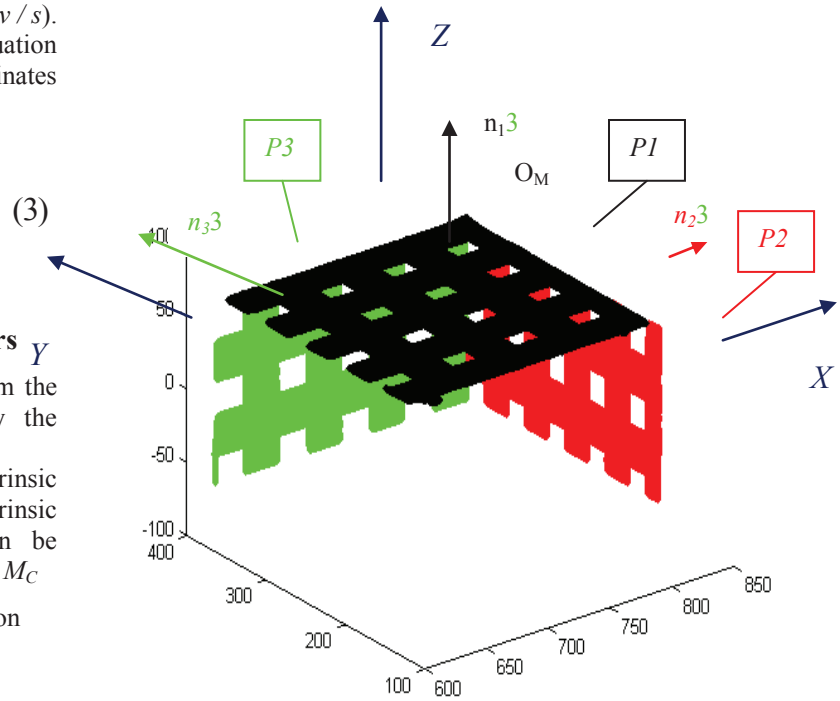


Figure 1 –Points cloud 3D calibration pattern obtained with the 3D scanner.

Plane must be perpendicular to the target. The least squares method, is used to calculate the normal vector to each plane, and the intersection of the three planes representing the origin of the coordinate of the target. The origin of the pattern allows us to compute the translation parameters of the transition matrix scanner. three normal vectors ( $n_1, n_2, n_3$ ) represents the rotation matrix. then It is possible to find the transformation matrix between the scanner and the 3D sights.

$$M_s = \begin{pmatrix} R & t \\ 0 & 1 \end{pmatrix} \quad (5)$$

### 3. Matching a CCD camera and a 3D laser sensor

We present in this paper a method for matching a CCD camera and a 3D laser sensor. As a first step, calibrate the devices located in the same space, due to the standard calibration techniques [5]. Then, calculate the transition matrix of the camera and the transition matrix of the 3D sensor. After that calculate the total transformation matrix  $M_t$  for combining the texture image obtained with the camera, and the surface obtained with the 3D scanner. This method is illustrated in Figure 2.1 and Figure 2.2, where for each vertex  $V_i$  point cloud obtained

with the scanner associating a pixel  $P_i$  of the image obtained with the camera.

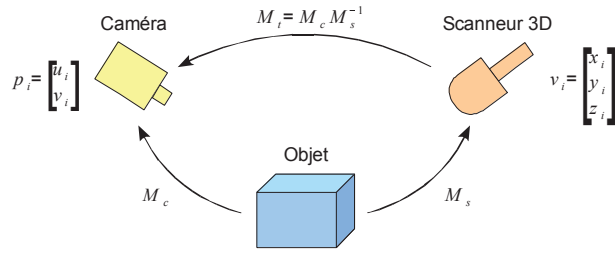


Figure 2.1 - Coupling of the camera and the 3D laser scanner

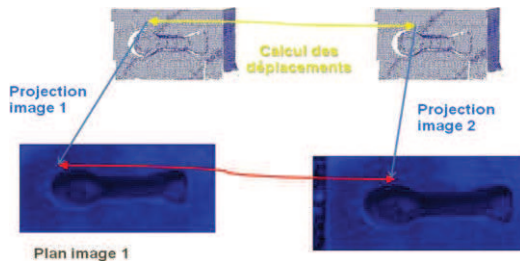


Figure 2.2 - Coupling of the camera and the 3D laser scanner

#### 4. MEASURING DIPLACEMENT

After calibration of the scanner and camera, we obtain an association between the pixel  $(u_i, v_i)$  of the camera image and the vertices  $(x_i, y_i, z_i)$  of the point cloud obtained with the scanner. At first, we acquire an object in an initial position, then move the object, and we repeat an acquisition. We select manually one characteristic point of the object before and after movement. In our experiment, the characteristic point is defined as a corner of a square of the calibration target. We find the coordinates  $(u, v)$  of the characteristic point in each image and then compute the coordinates  $(x, y, z)$  from the top of a scatter. Finally, we measure the displacement as the Euclidean distance between the 3D point feature found before and after displacement:

$$D = \sqrt{(x_2 - x_1)^2 + (y_2 - y_1)^2 + (z_2 - z_1)^2} \quad (6)$$

$$D_x = x_2 - x_1, \quad D_y = y_2 - y_1,$$

$$D_z = z_2 - z_1 \quad (7)$$

where  $(x_1, y_1, z_1)$  are the coordinates of the characteristic point on the scatter plot before displacement, and  $(x_2, y_2, z_2)$  coordinates of the characteristic points after displacement.

#### 5. RESULTS

In our experiment, we acquired with the 3D scanner and CCD camera of our calibration pattern in an initial position. Then we moved precisely the pattern along the x axis, and makes a new acquisition. The displacement is measured in an area defined manually using the method given in the previous section.

The following tables gives the results in terms of Euclidean distance and Dx: X-axis component of MMT, Dy: Y-axis component of the MMT, Dz: Z-axis component of the MMT calculated for each point associated with a pixel and the standard deviations obtained for each template 1, 5 and 7.

D: Euclidean distances

No	1	2	3	4	5	Standard Deviation
D <sub>image1</sub>	10.027	10.01	10.00	9.9901	9.980	0.0240
D <sub>image5</sub>	10.009	9.971	9.99	10.001	10.003	0.0269
D <sub>image7</sub>	9.997	9.964	9.99	9.987	9.999	0.0279

Dx: X-axis component of MMT.

No	1	2	3	4	5	Standard Deviation
Dx <sub>image1</sub>	-10.02	-10.009	-10.02	-9.99	-9.98	0.0234
Dx <sub>image5</sub>	-10.00	-9.97	-9.98	-9.99	-10.00	0.0266
Dx <sub>image7</sub>	-9.99	-9.98	-9.97	-9.98	-9.97	0.0238

Dy: Y-axis component of the MMT

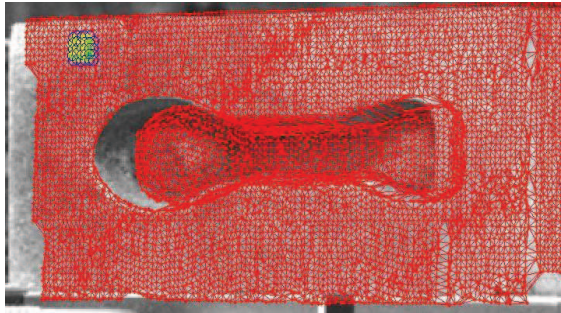
No	1	2	3	4	5	Standard Deviation
Dy <sub>image1</sub>	-0.256	-0.246	-0.234	-0.217	-0.201	0.021
Dy <sub>image5</sub>	-0.151	-0.122	-0.123	-0.136	-0.165	0.0229
Dy <sub>image7</sub>	-0.116	-0.008	-0.009	-0.0087	0.0093	0.0238

Dz: Y-axis component of the MMT

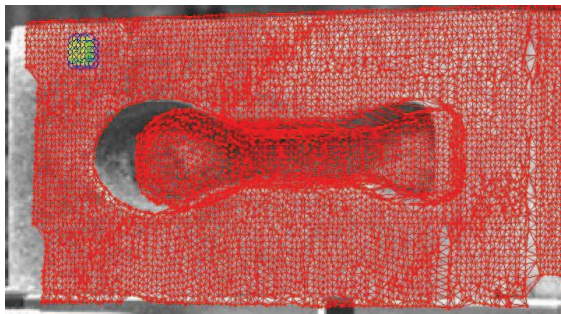


No	1	2	3	4	5	Standard Deviation
Dz <sub>imagette1</sub>	-0.253	0.250	0.246	0.243	0.239	0.0082
Dz <sub>imagette5</sub>	0.0048	-0.0051	-0.0054	-0.0056	-0.0062	0.0082
Dz <sub>imagette7</sub>	0.0088	0.0084	0.0082	0.0079	0.0076	0.0083

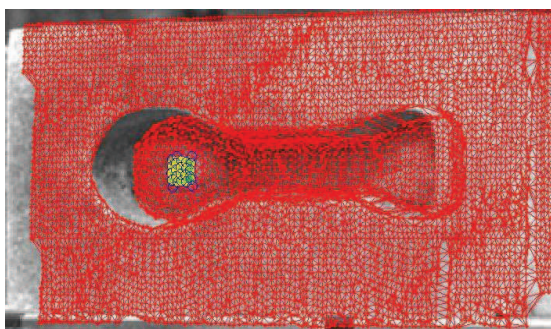
**Tables : Results obtained for each template 1, 5 and 7.**



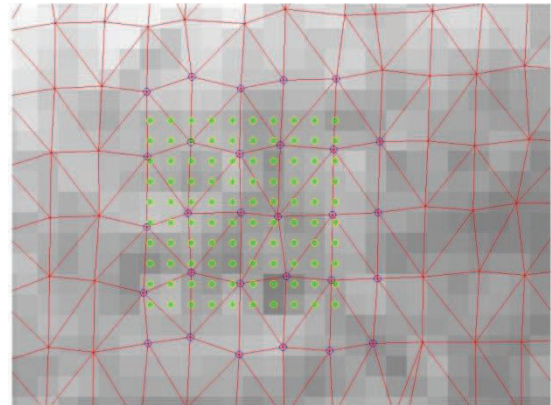
**template 1**



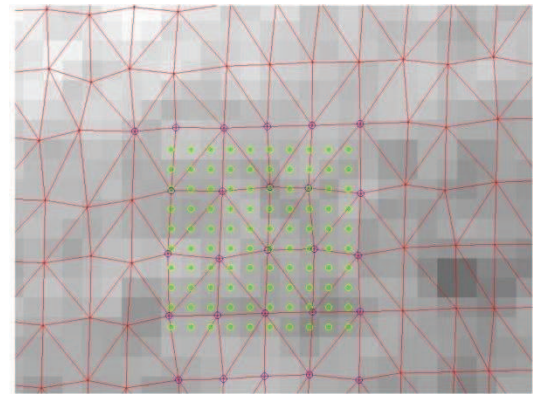
**template 5**



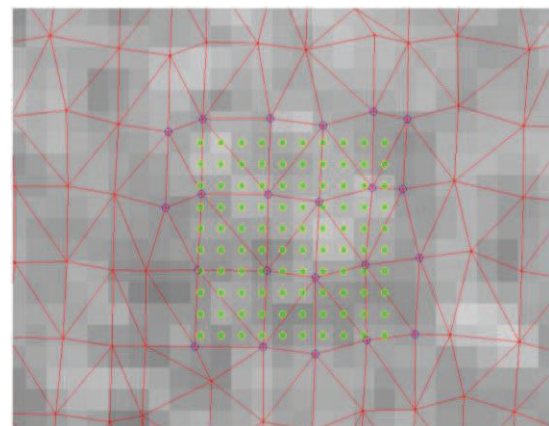
**template 7**



**template 1 before moving**

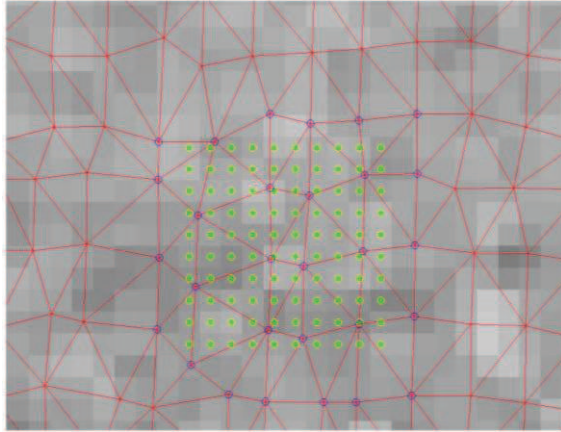


**template 1 after moving**

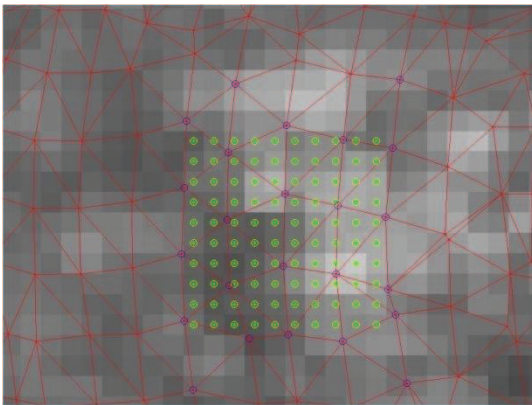


**template 5 before moving**

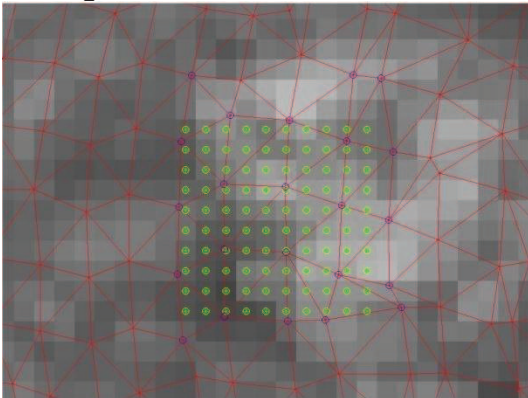
**Figure 3: The study area with the selected templates.**



template 5 after moving



Template7before  
moving



template 7 after moving

**Figure 4 :** Reason associated with the templates 1,2,7

We note that for the measured displacement is close to the specified motion. The standard deviations for each measurement or for a pattern of 100 in the directions X and Y are of the order of 0.02 mm and the Z-direction of about 0.01 mm. On a practical level, the movement being in a plane containing the optical axis and in a direction approximately equal to 45 ° with respect thereto. It is logical that the dispersion along the Z axis which is parallel to the image plane is smaller.

We also note that the results for 5 and 7 template, referring to surface and the other surface slightly left, are similar. against the differences between the results of these templates and template 1 may be explained by calibration errors. The use of a non-linear calibration matrix would correct errors due to optical distortions and significantly improve the result.

## 5. CONCLUSION

In this paper, we present a method for matching a CCD camera and a 3D laser sensor to obtain textured 3D model of an object observed. Then we proposed a method to calculate an estimate of the displacement using the point cloud and the image of the observed object present, we enhance this approach by automating the selection of areas measuring and controlling more finely calibration parameters. This work is part of an objective measurement of 3D deformation fields using the development tools.

## 6. REFERENCE

1. D.GARCIA,"Measuring shape and displacement fields dimensional stereo-image correlation," Ph.D. Thesis, Institut National Polytechnique de Toulouse, France, December 2001
2. D. Garcia, Orteu, JJ, Devy, M.: "Accurate Calibration of a Stereovision Sensor: Comparison of Different Approaches." 5 Visoin Workshop on Modeling, and Visualizaition 2000, Saarbrücken, Germany (2000)
3. D. Garcia, Orteu, JJ, Devy, M.: "precise calibration of a CCD camera or a stereoscopic vision sensor." LAAS Report No. 01332 Photpmécanique Symposium 2001, Poitiers, France (2001).
4. Frey, P. J. and George, P.-L. (1999). Meshes: application to finite elements. Hermes Science Publication.
5. G. CLOUD, "Optical methods of engineering analysis", Cambridge University Press, 1998
6. Kinsey, L. C. (1993). Topology of Surfaces. Springer-Verlag.
7. M.A.Sutton. The effects of subpixel picture restoration on digital correlation error estimates.Opt Eng 1988; 27 (3) :173-5
8. A.Sutton M., Wolters, W.J., Peters, W. H., Ranson, W.F., McNeill, S. R., 1983. Determination of displacements using digital correlation An improved method. Image and Vision Computing 1 (3) ,133-139.

9. M.A.Sutton, Cheng, M., Peters, W. H. Chao, Y.J., McNeill, S.R., 1986. Application of optimized digital correlation method year to planar deformation analysis. Image and Vision Computing 4 (3) ,143-150.
10. OD. Faugeras, G. Toscani, "Camera calibration for 3-D computer vision," Proceedings of IEEE International Workshop on Machine Vision years Machine Intelligence, Tokyo, Japan, 1987
11. O.D. FAUGERAS,, Toscani, G. "The calibration problem for stereo". In Proc. Computer Vision and Pattern Recognition, Miami Beach, Florida, USA, p.15-20 (1986).
12. R. . Horaud, Monga, O., "Computer Vision: basic tools (second edition)" Hermes (1995).
13. Spanier, E. H. (1981). Algebraic Topology. Springer-Verlag.
14. . S. YONEYAMA, A. KITAGAWA, S. IWATA, K. TANI, H. Kikuta, "Bridge deflection measurement using digital image correlation," Experimental Techniques, vol. 31, No. 1, p. 34-40, 2007
15. WH. PETERS, WF. Ranson, "Digital imaging techniques in experimental stress analysis," Optical Engineering, vol. 21, No. 3, p. 427-431, 1982